SL9 impact chemistry: Long-term photochemical evolution

By JULIANNE I. MOSES

Lunar and Planetary Institute, 3600 Bay Area Blvd., Houston, TX 77058-1113, USA

One-dimensional photochemical models are used to provide an assessment of the chemical composition of the Shoemaker-Levy 9 impact sites soon after the impacts, and over time, as the impact-derived molecular species evolve due to photochemical processes. Photochemical model predictions are compared with the observed temporal variation of the impact-derived molecules in order to place constraints on the initial composition at the impact sites and on the amount of aerosol debris deposited in the stratosphere. The time variation of NH_3, HCN, OCS, and H_2S in the photochemical models roughly parallels that of the observations. S_2 persists too long in the photochemical models, suggesting that some of the estimated chemical rates constants and/or initial conditions (*e.g.,* the assumed altitude distribution or abundance of S_2) are incorrect. Models predict that CS and CO persist for months or years in the jovian stratosphere. Observations indicate that the model results with regard to CS are qualitatively correct (although the measured CS abundance demonstrates the need for a larger assumed initial abundance of CS in the models), but that CO appears to be more stable in the models than is indicated by observations. The reason for this discrepancy is unknown. We use model-data comparisons to learn more about the unique photochemical processes occurring after the impacts.

1. Introduction

The Shoemaker-Levy 9 (SL9) impacts generated strong shocks in the jovian atmosphere in two distinct altitude regions: in the deep stratosphere or troposphere where strong deceleration of the comet fragments and maximum energy release occurred, and in the upper stratosphere where the impact plumes splashed back down into the atmosphere. Shocked, thermochemically processed cometary material and tropospheric jovian air were deposited in Jupiter's stratosphere after the impacts. The new impact-derived sulfur-, nitrogen-, oxygen-, and carbon-bearing molecules evolve with time due to solar ultraviolet photolysis, chemical reactions, vertical and horizontal transport, and condensation/aerosol formation. Because continuous observational coverage of the impact sites was not possible and because many of the potential impact-derived species are difficult to observe, photochemical models play an essential role in assessing the chemical state of the jovian atmosphere in the hours, days, and months following the impacts. We compare photochemical model predictions with observations in order to better define chemical abundances immediately after the impacts and to evaluate the long-term evolution of the impact-derived species.

The molecular species either detected for the first time in Jupiter's stratosphere or found to be enhanced after the SL9 impacts include S_2, CS_2, CS, OCS, NH_3, HCN, C_2H_4, H_2O, CO, and possibly H_2S (see Lellouch 1996). Of these observed species, S_2, OCS, H_2S, and NH_3 are found to be transient—observations taken months (and in some cases, days) after the impacts demonstrate that these molecules have disappeared or have been substantially reduced after the impacts (Noll *et al.* 1995, Yelle & McGrath 1996, Lellouch *et al.* 1995, Bézard *et al.* 1995, Griffith *et al.* 1995b, Fast *et al.* 1995). The signatures of two other molecules, CS_2 and CO, are observed to weaken over time, but spectra taken ~1 year after the impacts show evidence for the continued existence of both CS_2 and CO in the jovian stratosphere (McGrath *et al.* 1995, Matthews *et al.* 1995,

https://doi.org/10.1017/S0252921100115532 Published online by Cambridge University Press

R. Moreno *et al.* 1995). In contrast, spectral signatures for HCN and CS remain strong throughout the year following the impacts, indicating that the CS and HCN abundances have remained constant or even increased with time (R. Moreno *et al.* 1995, Matthews *et al.* 1995).

In the following sections, we describe how photochemical models can be used to simulate the evolution of these and other vapor-phase species at the impact sites; in particular, we recount the details of the photochemical models of Moses *et al.* (1995a,b,c). Because the models rely on accurate descriptions of the chemical state of the atmosphere just after the impacts, we also delve briefly into the details of some of the observations and theoretical predictions regarding the impact chemistry. More thorough discussions are presented in other chapters in this volume: observational results are reviewed by Lellouch (1996), and thermochemical models are described by Zahnle (1996). We then discuss the important photochemical reactions that control the abundances of the major observed species and compare model predictions with observational data.

2. Photochemical model: Initial conditions

Without accurate initial conditions, photochemical models cannot present a reasonable description of the time variation of the chemistry at the impact sites. Fortunately, observational coverage of the impact events was extensive. Unfortunately, complete spectral, temporal, and spatial coverage of each impact site was impossible. Different observations refer to different impact sites at different times and are sensitive to different altitudes; these issues must be considered carefully before initial chemical profiles can be developed. In addition, the impact and plume re-entry mechanics were complicated—different regions of the impact sites map back to diverse temperature and compositional regimes in the impact plume/fireball and hence probably contain different final compositions. Theoretical thermochemical models can help shed light on these issues, but they, too, are hampered by a lack of knowledge of physical and chemical conditions in the fireball and plume stages.

Moses *et al.* (1995a,b,c) have attempted to consider some of these complexities by splitting the photochemical modeling into two parts. First, Moses *et al.* (1995a,b) have created a model designed to reproduce the photochemical evolution in the dark central core region of an impact site (*e.g.*, a region that may contain fewer molecules derived from the comet). Then, (Moses *et al.* 1995c) have created a model designed to be more representative of extended regions of the impact sites, or the impact sites as a whole. The most obvious difference between the two models is that the dark-core model assumes a very low abundance of oxygen species while the whole-region model assumes a much higher abundance of oxygen species. As discussed below, the results of this splitting were not entirely satisfactory with regard to the actual situation on Jupiter, and better descriptions of the initial chemical state of the atmosphere at the impact sites should be possible now that more observational analyses are being published.

Table 1 shows the initial conditions assumed in the photochemical models. Column abundances at three different pressure levels are included to aid in comparisons with observations. For the dark-core low-oxygen case (hereafter called Model A), Moses *et al.* (1995a,b) assume that S_2 dominates the sulfur compounds, $N_2/NH_3/HCN \approx 10/10/1.6$, and oxygen compounds are very minor. For the whole-region high-oxygen case (Model C), Moses *et al.* (1995c) assume that most of the oxygen is tied up in CO, with $[H_2O] \approx 0.3[CO]$, $[OCS] \approx 6 \times 10^{-3}[CO]$, and minor additional amounts of SO_2 and CO_2 present. The sulfur and nitrogen abundances are taken from observations, except that N_2, S_2, and H_2S are assumed to be present in quantities (perhaps) greater than

	Model A Moses *et al.* (1995a,b)			Model C Moses *et al.* (1995c)		
Species	above 12 mbar	above 0.11 mbar	above 0.009 mbar	above 12 mbar	above 0.11 mbar	above 0.009 mbar
S_2	1.5×10^{18}	1.5×10^{17}	1.2×10^{16}	9.4×10^{16}	3.0×10^{16}	2.4×10^{15}
H_2S	7.7×10^{16}	7.4×10^{15}	6.1×10^{14}	2.0×10^{17}	7.4×10^{15}	6.1×10^{14}
CS	5.4×10^{11}	3.0×10^{10}	2.4×10^{9}	2.2×10^{14}	6.0×10^{13}	4.8×10^{12}
CS_2	2.0×10^{15}	1.8×10^{14}	1.5×10^{13}	7.9×10^{14}	2.2×10^{14}	1.8×10^{13}
N_2	1.5×10^{17}	1.5×10^{16}	1.2×10^{15}	7.1×10^{16}	2.2×10^{16}	1.8×10^{15}
NH_3	1.5×10^{17}	1.5×10^{16}	1.2×10^{15}	3.5×10^{17}	1.2×10^{16}	9.7×10^{14}
HCN	2.4×10^{16}	2.2×10^{15}	1.8×10^{14}	5.0×10^{15}	1.5×10^{15}	1.2×10^{14}
H_2O	1.8×10^{14}	1.5×10^{13}	1.2×10^{12}	1.4×10^{18}	4.5×10^{17}	3.6×10^{16}
CO	1.8×10^{14}	1.5×10^{13}	1.2×10^{12}	4.0×10^{18}	1.3×10^{18}	1.1×10^{17}
CO_2	2.3×10^{12}	1.5×10^{11}	1.2×10^{10}	3.8×10^{12}	6.0×10^{11}	4.8×10^{10}
SO_2	1.0×10^{13}	7.4×10^{11}	6.1×10^{10}	3.1×10^{13}	7.4×10^{12}	6.0×10^{11}
OCS	2.3×10^{12}	1.5×10^{11}	1.2×10^{10}	2.4×10^{16}	7.4×10^{15}	6.1×10^{14}

TABLE 1. Initial column abundances (molecules cm^{-2})

observed, and their abundances are estimated by assuming a comet-like O/S/N ratio of roughly 25/2/1 (see Lellouch 1996) in the upper stratosphere ($P < 0.3$ mbar). Additional amounts of NH_3 and H_2S are assumed to be present in the lower stratosphere ($P > 0.3$ mbar) based on the suggestions of Yelle & McGrath (1996). Initial conditions for both of these models are out-of-date and need to be updated based on new observational and theoretical analyses.

2.1. *Constraints based on observations*

Moses *et al.* (1995a,b,c) selected initial abundances for their photochemical models in such a way as to remain as consistent as possible with the available observational reports. A thorough and detailed discussion of the observations is presented in Lellouch (1996). We will not attempt to repeat that information here but will simply provide a summary of some of the sources of the observational constraints. Table 2 contains a list of several early papers that have been particularly useful in constraining initial abundances for the photochemical models. Along with the observed molecules listed in this table, useful upper limits to many additional species are presented by Noll *et al.* (1995), Lellouch *et al.* (1995), Atreya *et al.* (1995), Yelle & McGrath (1996), Caldwell *et al.* (1995), and Sprague *et al.* (1996).

The observations of the chemical species taken at different wavelengths with different instruments are occasionally inconsistent; even within one dataset (*e.g.*, the Hubble Space Telescope ultraviolet spectra), different investigators derive dissimilar results. The inconsistencies probably derive from the different assumptions that have gone into the observational analyses. The major stumbling blocks to deriving chemical abundances are uncertainties about the stratospheric temperatures (for the infrared and even millimeter and sub-millimeter observations) and uncertainties about the absorbing properties of the aerosols (for the ultraviolet observations). However, most of the recent reports appear to exhibit a convergence with regard to chemical abundances (see Lellouch 1996), and it is hoped that these results can be used to place robust constraints on the initial conditions for the photochemical models.

Species	References used to constrain initial conditions
S_2	Noll *et al.* (1995), Yelle & McGrath (1996)
H_2S	Atreya *et al.* (1995), Caldwell *et al.* (1995), Noll *et al.* (1995), Yelle & McGrath (1996)
CS	Lellouch *et al.* (1995), R. Moreno *et al.* (1995), Noll *et al.* (1995)
CS_2	Atreya *et al.* (1995), Caldwell *et al.* (1995), McGrath *et al.* (1995), Noll *et al.* (1995), Yelle & McGrath (1996)
NH_3	Atreya *et al.* (1995), Betz *et al.* (1995), Bézard *et al.* (1995), Caldwell *et al.* (1995), Conrath *et al.* (1995), Fast *et al.* (1995), Griffith *et al.* (1995a,b), Kostiuk *et al.* (1996), McGrath *et al.* (1995), Noll *et al.* (1995), Orton *et al.* (1995), Yelle & McGrath (1996)
HCN	Griffith *et al.* (1995a), Marten *et al.* (1995), Matthews *et al.* (1995)
H_2O	Bjoraker *et al.* (1995), Carlson *et al.* (1995), Cosmovici *et al.* (1995), Meadows & Crisp (1995), Sprague *et al.* (1996)
CO	Brooke *et al.* (1995), Knacke *et al.* (1995), Lellouch *et al.* (1995), Maillard *et al.* (1995), Matthews *et al.* (1995), R. Moreno *et al.* (1995)
OCS	Lellouch *et al.* (1995)

TABLE 2. *Sources of observational constraints*

2.2. *Constraints based on thermochemical modeling*

When observations are unavailable, uncertain, or contradictory, theoretical models of the thermochemical processing that takes place in the fireball, plume, and plume re-entry shock can be used to help determine the initial chemical composition of the impact sites. Thermochemical models such as those presented by Zahnle (1996), Zahnle *et al.* (1995), Lyons & Kansal (1996), and Borunov *et al.* (1995) that predict how the different elements are partitioned among their constituent molecules are particularly useful in estimating the abundances of species that are difficult or impossible to observe on Jupiter. For example, molecular nitrogen is not observable in the jovian stratosphere, but theoretical models (*e.g.*, Zahnle 1996, Lyons & Kansal 1996) predict that it should be a major product under most shock pressure/temperature regimes relevant to the impacts. Similarly, H_2O is difficult to observe once it has cooled to ambient stratospheric temperatures; therefore, the observed H_2O abundance (*e.g.*, Bjoraker *et al.* 1995, Sprague *et al.* 1996) may represent a lower limit. Because H_2O photolysis drives the oxygen photochemistry, estimating its initial abundance is important for photochemical models. Thermochemical models are useful not only for supplying the photochemical models with initial conditions, but also for helping to determine the elemental compositions of the comet and/or jovian troposphere and for constraining the physical conditions of the impacts.

The temperatures and pressures in the fireball and re-entry shock play a critical role in determining the chemical makeup at the impact sites (cf. Zahnle 1996, Lyons & Kansal 1996). Although infrared observations are used to pin down the shock temperatures during plume re-entry (*e.g.*, Kim *et al.* 1995), the conditions in the initial shock are less certain. Numerical models of the impacts can help with this task. Zahnle (1996) uses hydrodynamic plume models to define the physical conditions for his thermochemical modeling; however, he finds that different gas parcels experience very different thermal histories depending on where they were positioned during the initial shock. Currently, no one has "added up" the different parcels in such a way as to map out compositional changes at the impact sites (due to different shock conditions) so that a three-dimensional description of the impact-site composition can be developed.

Even more important to the thermochemical models may be the relative elemental abundances in the plume/fireball; in particular, the C/O ratio controls much of the thermochemistry. For moderate or high shock temperatures, Zahnle (1996) and Lyons & Kansal (1996) show that plumes with C/O > 1 allow most of the oxygen to be tied up in CO, with H_2O, SO_2, SiO, NO, and SO playing a minor role; the excess carbon can then be used to form species such as carbon sulfide and hydrocarbons. Plumes with C/O < 1 have H_2O being more important than in the C/O > 1 case, C–S species being minor, and SO and SO_2 becoming increasingly important as shock temperatures become higher. What was the C/O ratio in the plumes during the SL9 impacts? That question may not be a reasonable one to ask because different portions of the plume may have contained different elemental compositions due to a variable amount of mixing between the vaporized comet and jovian air. Observations are somewhat contradictory regarding this point. Both H_2O and OCS were observed in non-trivial quantities, suggesting that C/O < 1. However, CS and CS_2 were also observed in moderate quantities while SO_2 is not reported, suggesting that C/O > 1. The problem is clearly complex. We seem to be seeing more than one type of chemistry in different regions of the impact sites. Until model parameter space has been explored more fully and until the observational constraints become increasingly secure, the initial conditions at the impact sites will remain uncertain.

3. Photochemical model: Other details

Moses *et al.* begin their modeling approximately one half hour after the impacts, after the plumes have splashed back down and spread into the upper atmosphere and after the surrounding air has cooled to a significant degree. Thermochemical processes cease to dominate the chemistry at this point, and solar radiation takes over. The models are one-dimensional in the vertical direction. Molecular and eddy diffusion are considered, but horizontal spreading is neglected. Because of this and other oversimplifications, the models are designed to illustrate general trends in the evolutionary behavior of the molecules introduced by the impacts; the results should be regarded as illustrative rather than quantitative.

The photochemical models simulate the variation of 145 different vapor-phase sulfur, nitrogen, oxygen, and hydrocarbon compounds at the impact sites. Over 900 chemical reactions are included. Most of the reaction rates are taken from the NIST Chemical Kinetics Database (version 6.0, Mallard *et al.* 1994) and literature published within the last couple of years; however, several potentially important reactions used in the model have never been studied in the laboratory. Moses *et al.* estimated the pathways, rates, and products for these reactions. The sulfur reactions, in particular, are poorly studied. A complete reaction list is available from J. Moses upon request.

The background atmosphere, temperature profile, and diffusion coefficients of Gladstone *et al.* (1996) are used in the photochemical models. Solar flux values from 1983 data are used in Model C; values from 1980 data, which are probably higher than those relevant to the 1994 impact date, are used in Model A. The exact choice of solar flux does not significantly affect the results because much of the photochemistry is initiated by longer wavelength ultraviolet radiation that does not vary noticeably with the solar cycle. The fluxes are diurnally averaged for 44° S latitude using the Jupiter-Sun geometry at the time of the impacts. A steady-state model that just considers hydrocarbon photochemistry is first created to simulate the pre-impact atmosphere. The resulting hydrocarbon-species profiles are then used as initial conditions for the post-impact model.

For boundary conditions, zero flux is assumed for all species except atomic H at the top of the atmosphere (10^{-6} mbar) and a zero concentration gradient at the bottom (6 bar) so that the species flow into the troposphere at a maximum possible rate. Atomic hydrogen, which is produced in the thermosphere of Jupiter, is given a downward flux of 4×10^9 cm^{-2} s^{-1} at the top (see Gladstone *et al.* 1996). Because the impact-derived species are not being continually replenished in the stratosphere, they will eventually diffuse or rain out into the troposphere. The eddy diffusion time scale at 1 mbar is 5 years for the unperturbed stratosphere but may be shorter at the impact sites if the events stirred up the atmosphere to any degree. Condensation is not included explicitly in the Moses *et al.* models, but potential condensates are noted.

4. Photochemical model: Results

The photochemical models of Moses *et al.* (1995a,b,c) demonstrate that the post-SL9 jovian stratosphere is a very dynamic place, with chemical abundances changing on time scales ranging from minutes to years. In the following sections, we will discuss the major photochemistry results in terms of the fate of the sulfur-, nitrogen-, and oxygen-bearing molecules. Although the initial conditions adopted in these early models are unlikely to be correct from a quantitative standpoint, the qualitative results can be used to illuminate the behavior of several of the observed species and to make predictions concerning the long-term evolution of the major impact-derived molecules. We will also use the models to identify molecular species that are photochemically stable and can be used to trace temperature changes or atmospheric dynamics, to identify molecules that might condense and affect atmospheric haze properties, to identify important as-yet-unobserved molecular species, and to use the predicted temporal variation in conjunction with observations to learn more about the unique photochemical processes occurring in the post-SL9 jovian stratosphere.

4.1. *Sulfur*

The photochemistry of sulfur in a reducing atmosphere is poorly understood. Very few rate constants are available in the literature, and Moses *et al.* were forced to estimate the rates for several important reactions. The best-studied reactions are those of sulfur compounds with sulfur, oxygen, and some hydrocarbon species. Significantly absent are reactions of sulfur species with organic radicals and nitrogen species, and possible formation mechanisms for sulfanes (H_2S_x). Despite uncertainties in reaction rates and initial conditions, one robust conclusion can be surmised from the photochemical models: the ultimate sink for the sulfur compounds is condensed S_8. Figures 1 and 2 illustrate the time variation in the partitioning of the sulfur compounds in the dark-core (Model A) and whole-disk (Model C) models.

Although many sulfur molecules were detected after the impacts, their relative abundances are not well known due to difficulties with the observational analyses. One very important molecule, both because of its high initial abundance and its low photochemical stability, is diatomic sulfur (S_2). Because of its short lifetime under laboratory conditions, S_2 has not been well studied. In the photochemical models, S_2 is lost due to rapid photolysis in the upper atmosphere and to the formation of larger sulfur molecules in the lower stratosphere. The S_2 (B–X) band system lies at 240–360 nm and is clearly observed by the Hubble Space Telescope (HST) Faint-Object Spectrograph (FOS) (Noll *et al.* 1995, Yelle & McGrath 1995). At wavelengths shorter than ~278 nm, the S_2 dissociates into two ground-state (^3P) sulfur atoms. The diurnally averaged lifetime against photolysis for the S_2 molecule at 10^{-3} mbar and 44° S latitude on Jupiter is ~6 hours.

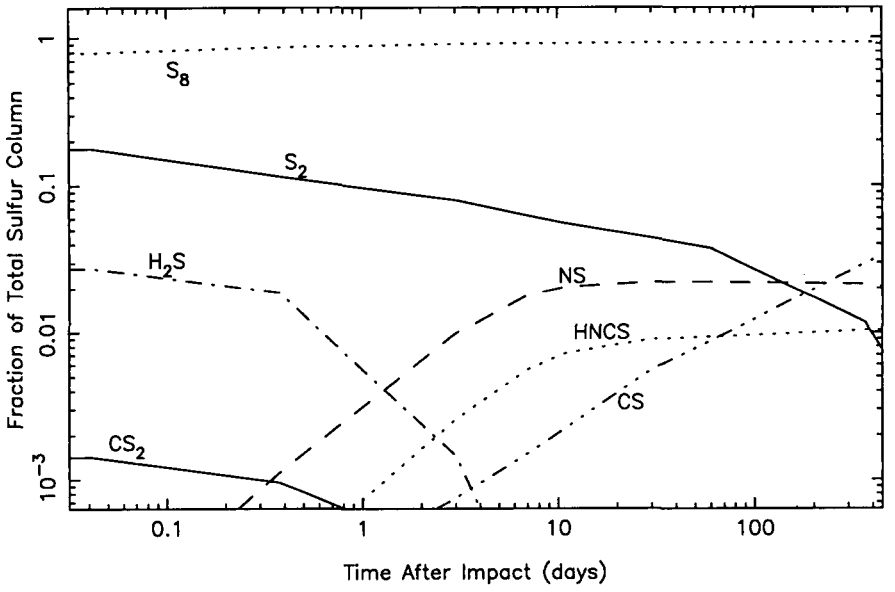

FIGURE 1. The time variation of the partitioning of sulfur compounds in Model A (Moses *et al.* 1995a). The ordinate represents the fraction of the total sulfur column (in terms of S atoms) that is contributed by the various molecules.

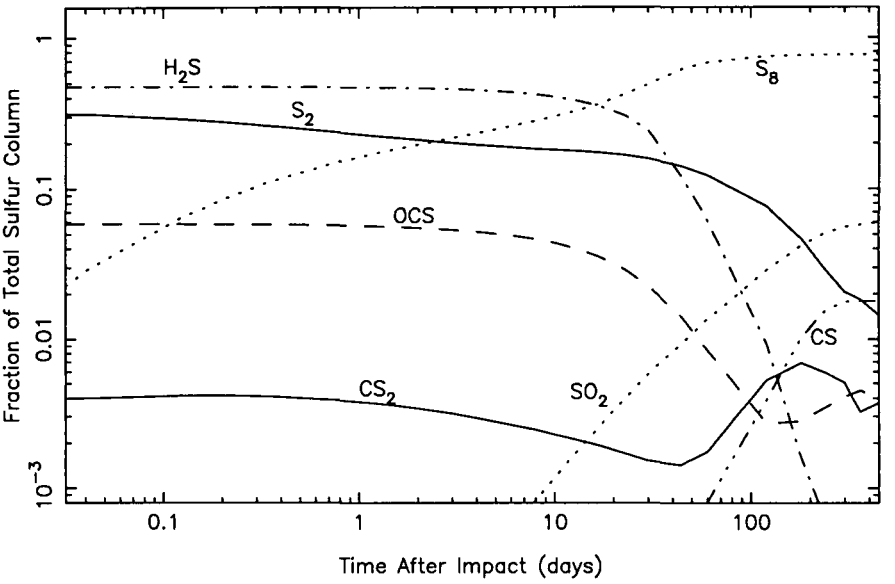

FIGURE 2. The time variation of the partitioning of sulfur compounds in Model C (Moses *et al.* 1995c). The ordinate represents the fraction of the total sulfur column (in terms of S atoms) that is contributed by the various molecules. Not shown, but also important sulfur reservoirs at various times, are S, S_3, S_4, H_2S_4, SO, $(SO)_2$, S_2O, NS, and HNCS.

https://doi.org/10.1017/S0252921100115532 Published online by Cambridge University Press

Ground-state $S(^3P)$ atoms do not insert into H_2 or alkanes (*e.g.*, CH_4 and C_2H_6), but they do insert into alkenes (*e.g.*, C_2H_4) and alkynes (*e.g.*, C_2H_2) to form ring species that are stable in the former case and transient in the latter case. However, if S_2 is as abundant as Yelle & McGrath (1995) indicate (*e.g.*, 5×10^{15} cm^{-2}), the most probable fate of the sulfur atoms is to recycle S_2. Chemical loss processes other than photolysis dominate the loss of S_2. The major sink for S_2 in the photochemical models is the production of molecular sulfur (S_8) via a variety of three-body and other reactions:

$$\begin{aligned}
S_x &\xrightarrow{h\nu} S_{x-1} + S && \text{for } x = 2, 3, 4\\
2S &\xrightarrow{M} S_2\\
S + S_2 &\xrightarrow{M} S_3\\
2S_3 &\xrightarrow{M} S_6\\
S_2 + S_x &\xrightarrow{M} S_{x+2} && \text{for } x = 2, 4, 6\\
S + S_x &\longrightarrow S_2 + S_{x-1} && \text{for } x = 3, 4, 5, 6\\
2S_4 &\xrightarrow{M} S_8
\end{aligned}$$

where M represents any third molecule or atom and $h\nu$ represents an ultraviolet photon. The S + S and $S_2 + S_2$ three-body reactions have been found to be extremely rapid in the laboratory (*e.g.*, Nicholas *et al.* 1979); the other three-body rates have not been measured, and Moses *et al.* conservatively adopt rates that are lower than that for S_2+S_2. Even so, the formation of S_8 proceeds extremely rapidly in the lower stratosphere. Over 70% of the initial column budget of S_2 molecules in Model A has been converted to S_8 in the first hour of the calculations, and another $\sim$ 10% is converted to other sulfur molecules during the same time period. S_8 has a low volatility and will condense almost as soon as it is formed.

Because the reaction $2S_2 \xrightarrow{M} S_4$ dominates the loss of S_2 in the stratosphere, the rate of loss is dependent on the initial S_2 abundance. Moses *et al.* start with 16 times less S_2 in Model C than they do in Model A, so the rate of conversion of S_2 to other sulfur molecules in Model C is much slower (cf. figures 1 & 2). However, neither model has S_2 molecules being lost as quickly as one might expect. Rapid photolysis of S_3 and S_4 ensures efficient recycling of the S_2 by the following scheme:

$$\begin{aligned}
2(2S_2 &\xrightarrow{M} S_4)\\
S_4 &\xrightarrow{h\nu} S_3 + S\\
S_3 &\xrightarrow{h\nu} S_2 + S\\
S + S_3 &\longrightarrow 2S_2\\
S + S_4 &\longrightarrow S_2 + S_3\\
\hline
&\text{Net: nothing}
\end{aligned}$$

This recycling scheme allows S_2 to persist in the middle stratosphere in the photochemical models despite rapid loss mechanisms. Remember, however, that the Moses *et al.* models are diurnally averaged. On Jupiter, the situation may be different. Recycling of S_2 at the impact sites will be very efficient until the sites rotate beyond the evening terminator. Once photons are no longer available to dissociate the S_2, S_3, and S_4 molecules, formation of S_8 will proceed uninhibitedly. Therefore, the diurnally averaged models may considerably overestimate the S_2 abundance after a full Jupiter rotation. Future models should allow diurnal variation. In addition, the S_2 may have been deposited higher in the atmosphere and be at a higher temperature (Yelle & McGrath 1995) than has been assumed in the photochemical models. In that case, the formation of S_8 and other large sulfur molecules will be inhibited.

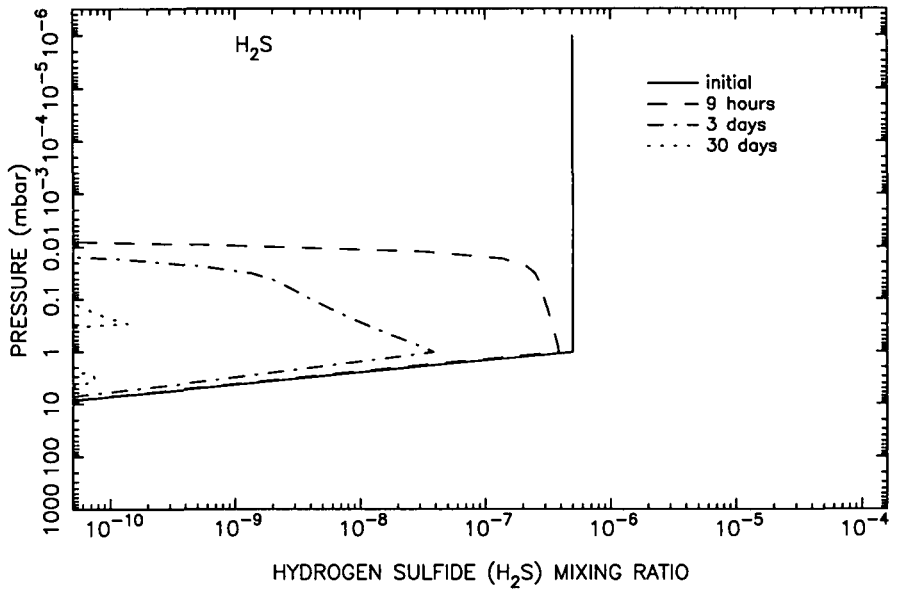

FIGURE 3. The photochemical evolution of H_2S in Model A (from Moses *et al.* 1995a) in terms of the temporal variation of the H_2S mixing ratio profile.

Hydrogen sulfide (H_2S) has been inferred from the July 18 HST FOS spectra of the G impact site (Noll *et al.* 1995, Yelle & McGrath 1996) because of the presence of a broad absorption feature in the 180–210 nm region. However, this spectral signature is not unique to H_2S; Atreya *et al.* (1995) suggest that the absorption slope in this wavelength region is due to aerosols rather than to H_2S (although they, too, seem to include H_2S in their modeling). There are many reasons why one might expect hydrogen sulfide to be present after the impacts. Thermochemical models (*e.g.*, Zahnle 1996, Lyons & Kansal 1996) show that H_2S tends to form under similar shock temperature and pressure conditions as NH_3, and NH_3 was observed to be enhanced in the jovian stratosphere after the SL9 impacts. If the comet fragments penetrated to at least the putative NH_4SH clouds and/or if sulfur was present in the comet in a solar-type abundance, then Zahnle (1996) and Lyons & Kansal (1996) predict that H_2S will be present after the plume splashdown in regions in which plume re-entry temperature did not exceed 2000 K (*e.g.*, near the central region of the plume re-entry scars). Similarly, if the bulk of the NH_3 comes from a later "upwelling" of tropospheric material, as Yelle and McGrath (1996) and others have suggested, then one might also expect H_2S to be present along with the NH_3. Because of these theoretical predictions, Moses *et al.* (1995a,b,c) have included H_2S in their photochemical models, and have even added "extra" H_2S in the lower stratosphere in Model C based on Yelle & McGrath's suggestion that the bulk of both the ammonia and hydrogen sulfide may be located at pressures greater than 5 mbar. Because the presence of H_2S is not clear-cut, both models may greatly overestimate the initial abundance of hydrogen sulfide.

The photochemical models demonstrate that H_2S has a very short lifetime in the jovian stratosphere (see figure 3). The H_2S lifetime against photolysis is $\sim$2 days at 10^{-3} mbar. H_2S is also lost from the upper atmosphere by reaction with atomic hydrogen; both processes act to remove H_2S from the upper atmosphere on time scales of hours. The SH

https://doi.org/10.1017/S0252921100115532 Published online by Cambridge University Press

formed from the H_2S loss processes does not act to recycle the H_2S. In the middle and upper stratosphere, H_2S photochemistry can be reduced to the following simple scheme:

$$\begin{aligned} H_2S &\xrightarrow{h\nu} SH + H \\ H_2S + H &\longrightarrow SH + H_2 \\ SH + H &\longrightarrow H_2 + S \\ SH + S &\longrightarrow S_2 + H \\ \hline \text{Net: } 2H_2S &\longrightarrow 2H_2 + S_2 \end{aligned}$$

The above scheme, which operates rapidly in the jovian stratosphere, shows that the H_2S photolysis products act to increase the budget of the elemental sulfur molecules in the atmosphere.

Moses *et al.* (1995c) find that in Model C, H_2S can persist in the lower stratosphere if UV-absorbing dust is present to act as an effective shield against photolysis. Because H_2S photolysis is the primary source of H atom production at altitudes below 0.1 mbar, both loss mechanisms described in the above scheme are inhibited by dust shielding. In both photochemical models, however, the H_2S is eventually removed from the stratosphere (cf. figures 1 & 2).

Hydrogen tetrasulfide (H_2S_4) and other sulfanes (H_2S_x) are produced in minor quantities as result of H_2S and S_2 photolysis. When SH reacts with sulfur radicals such as S_3 and S_4, HS_2 is formed. Two HS_2 molecules can react along with a stabilizing third molecule or atom to form H_2S_4. However, this process is not the dominant loss mechanism for HS_2 in the photochemical models, and H_2S_4 and H_2S_x never become very abundant. H_2S_4 and H_2S_x are relatively involatile and can condense in the jovian stratosphere.

Carbon disulfide (CS_2) is observed unambiguously in the HST FOS spectra (Noll *et al.* 1995, Atreya *et al.* 1995, Yelle & McGrath 1996). Both Yelle & McGrath (1996) and Atreya *et al.* (1995) derive CS_2 column abundances of $\sim 10^{15}$ cm^{-2}. CS_2 has strong (resolved) absorption bands in the 185–230 nm region. At these wavelengths, the dissociation pathway is CS + S, with $\sim$ 80% of the sulfur atoms being formed in the ^{1}D excited state and the rest in the ^{3}P ground state (Yang *et al.* 1980). The S(^{1}D) will then react with H_2 to produce SH + H and the SH reacts to reform S and S_2. CS_2, like S_2, is recycled in the middle or lower stratosphere and is not lost as fast as its photolysis rate ($\sim$ 9 hours at 10^{-3} mbar) would indicate. Instead, the CS produced from CS_2 photolysis can react with S_2 or SH to recycle CS_2. On the other hand, photolysis is effective at removing CS_2 from the upper stratosphere (*e.g.*, $P < 10^{-3}$ mbar in Model A or 10^{-2} mbar in Model C). The late increase in the CS_2 abundance shown in figure 2 is due to reactions of sulfur and hydrocarbon radicals (see the CS discussion below).

Carbon monosulfide (CS) is a primary thermochemical product in the plume splashdown if the C/O ratio in the plume is grater than unity (Zahnle 1996, Lyons and Kansal 1996). CS is also produced directly by CS_2 photolysis and indirectly by several different reaction schemes whose ultimate source revolves around S_2. Laboratory studies of CS indicate that it is a short-lived radical that seems to self-polymerize rapidly (Moltzen *et al.* 1988). However, this polymerization reaction, which is not well understood, seems to require the presence of a container wall or other solid surface. Moses *et al.* (1995a,b,c) therefore concluded that CS might not polymerize in Jupiter's atmosphere (unless the reactions could somehow take place on aerosol surfaces) and so did not include polymerization schemes for CS. The apparent long lifetime of CS in the jovian stratosphere (R. Moreno *et al.* 1995) seems to have justified this conclusion.

Although Moses *et al.* (1995a,b,c) did not begin with much CS in their models, they found that the modeled CS abundance increases dramatically with time. The CS pho-

tochemistry is complex and difficult to follow, but it appears that reactions of S_2 and S with hydrocarbon radicals are responsible for the delayed increase in abundance shown in figures 1 & 2. The greater the initial S_2 abundance, the more CS that will be produced. Several reaction schemes such as the following contribute to CS production in the months following the impacts:

$$\begin{aligned} S_2 + C_2H_3 &\longrightarrow HCS + H_2CS \\ HCS + H &\longrightarrow CS + H_2 \\ H_2CS &\xrightarrow{h\nu} CS + H_2 \\ \text{Net: } S_2 + C_2H_3 + H &\longrightarrow 2CS + 2H_2 \end{aligned}$$

This scheme is the dominant source of CS production in both Model A & C. A similar scheme involving $S + CH_3 \longrightarrow H_2CS + H$ is also important in Model A. The low abundance of C_2H_3 and the relatively slow estimated rate for $S_2 + C_2H_3$ cause a delay in the production of CS by this and other similar mechanisms, especially in Model C, which has a smaller initial S_2 abundance. Note that thioformaldehyde (H_2CS) is an important intermediate in most of the schemes that convert S and S_2 into CS and CS_2 in the late stages of the sulfur photochemistry. The H_2CS abundance increases noticeably within a week of so after the impacts in the photochemical models, but its predicted peak column abundance (10^{14}–10^{15} cm^{-2}) may not be sufficient to allow H_2CS to be observable. Other organo-sulfur molecules such as methyl mercaptan (CH_3SH) and ethylene episulfide (C_2H_4S) are predicted to be even less abundant than H_2CS.

Because the limited available laboratory data indicate that CS reactions with other radical species are relatively slow, Moses *et al.* (1995a,b,c) find that very few reactions seem to be effective at removing CS from Jupiter's stratosphere. The only reactions that permanently remove CS from the modeled atmosphere are the hypothetical reactions $NH_2 + CS \longrightarrow HNCS + H$ and $CS + SO \longrightarrow S + OCS$; all others tend to recycle the CS. Moses *et al.* estimate relatively small rate constants for both these unmeasured reactions; however, both reactions eventually become important.

Once NH_3 photolysis begins, nitrogen-sulfur species become important reservoirs for both sulfur and nitrogen in the photochemical models. This result is highly speculative because very few kinetic studies of reactions between sulfur and nitrogen radicals are available in the literature. The two main nitrogen-sulfur molecules in the photochemical models, nitrogen sulfide (or sulfur nitride, NS) and isothiocyanic acid (HNCS) have both been detected in interstellar space (Turner 1989). Under laboratory conditions on Earth, NS (like CS) is a radical species that tends to polymerize rapidly (Heal 1972). In Jupiter's stratosphere, NS polymerization may not be as important, and photolysis or reactions such as $NH_2 + NS \longrightarrow N_2 + H_2S$ may be responsible for NS loss. In the photochemical models, NS is produced by $NH_2 + S \longrightarrow HNS + S$ followed by HNS photolysis or $HNS + S \longrightarrow NS + SH$. Photolysis of NS supplies a source of N atoms to the jovian stratosphere.

As already mentioned, Moses *et al.* find that HNCS is produced by the reaction of NH_2 with CS. Photolysis is the dominant loss mechanism—HNCS has a strong absorption band in the 210–270 nm region. However, if the dissociation pathway is predominantly H + NCS, the HNCS is likely to be recycled. Figure 1 shows that the abundances of NS and HNCS increase dramatically with time in Model A; these species also increase with time in Model C, but the NS and HNCS curves were deleted from figure 2 to keep the figure from becoming too confusing.

Carbonyl sulfide (OCS), which was detected at millimeter wavelengths by Lellouch *et al.* (1995), has a photolysis lifetime of $\sim$ 24 days at 10^{-3} mbar. The predominant photodissociation pathway is $CO + S(^1D)$. Recycling of OCS does not occur in the photochemical models; however, some OCS production takes place by the reaction CS

https://doi.org/10.1017/S0252921100115532 Published online by Cambridge University Press

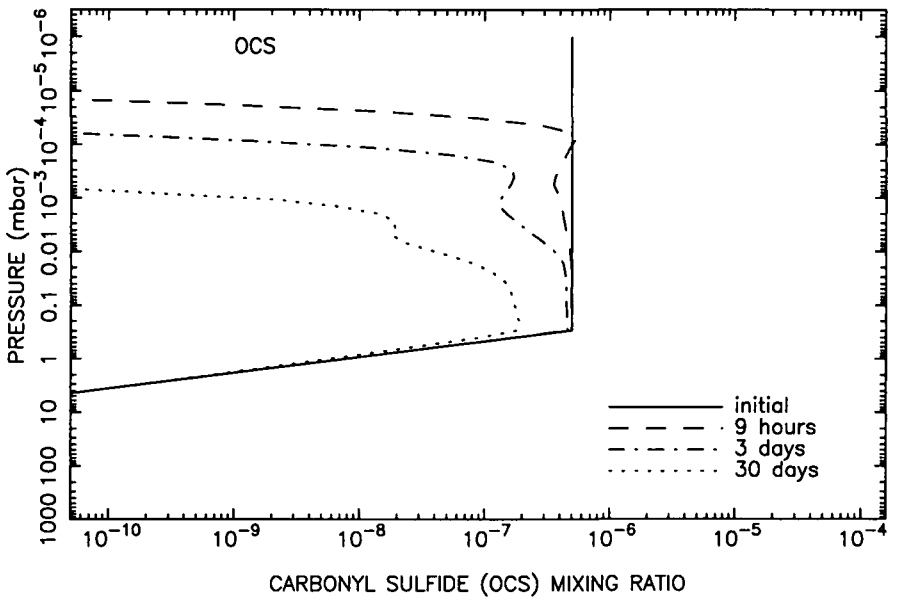

FIGURE 4. The photochemical evolution of OCS in Model C (from Moses *et al.* 1995c) in terms of the temporal variation of the OCS mixing ration profile.

+ SO $\longrightarrow$ OCS + S, thus increasing the apparent OCS lifetime. Figure 4 shows the variation of the OCS mixing ratio with time in Model C. Note that OCS is more stable against photolysis in the middle and upper atmosphere than H_2S, CS_2, or S_2.

Sulfur dioxide (SO_2) and sulfur monoxide (SO) are also important reservoirs for the sulfur in models in which the initial water abundance is high (see figures 2 & 5). In fact, SO_2 is responsible for 5.8% and SO for 2.5% of the total column of sulfur after 1 year in Model C. SO and SO_2 formation depend on H_2O photolysis. Water photodissociates primarily into OH + H, and the OH radicals react with atomic sulfur to form SO, which can then react with itself to form SO_2 + S. Although the chemical rate constants and other input parameters to the photochemical models are uncertain, any late build up in the SO_2 abundance observed in the jovian stratosphere long after the impacts would most certainly be due to H_2O photolysis; therefore, a detection or even upper limit on the SO_2 abundance many months after the impacts would greatly aid in constraining the water abundance (if the measured H_2O abundance is indeed a lower limit).

Most of the sulfur molecules produced after the impacts are volatile enough or not abundant enough to condense in the models. Exceptions are S_8, H_2S_4, and other sulfanes (H_2S_x). Elemental sulfur, in particular, should be condensing proliferously about any pre-existing aerosols if S_2 was at all an important component at the impact sites.

4.2. *Nitrogen*

The kinetics of nitrogen compounds in a reducing atmosphere are much better studied than the corresponding case for sulfur, and Moses *et al.* (1995a,b,c) were able use laboratory measurements of reaction rates for most of the nitrogen reactions in their model. The nitrogen compounds formed during the SL9 impacts tend to be more stable than the sulfur compounds. In fact, of the three major nitrogen species introduced by the impacts—ammonia (NH_3), hydrogen cyanide (HCN), and molecular nitrogen (N_2)—only ammonia is photochemically active. Thus, NH_3 drives the nitrogen photochemistry

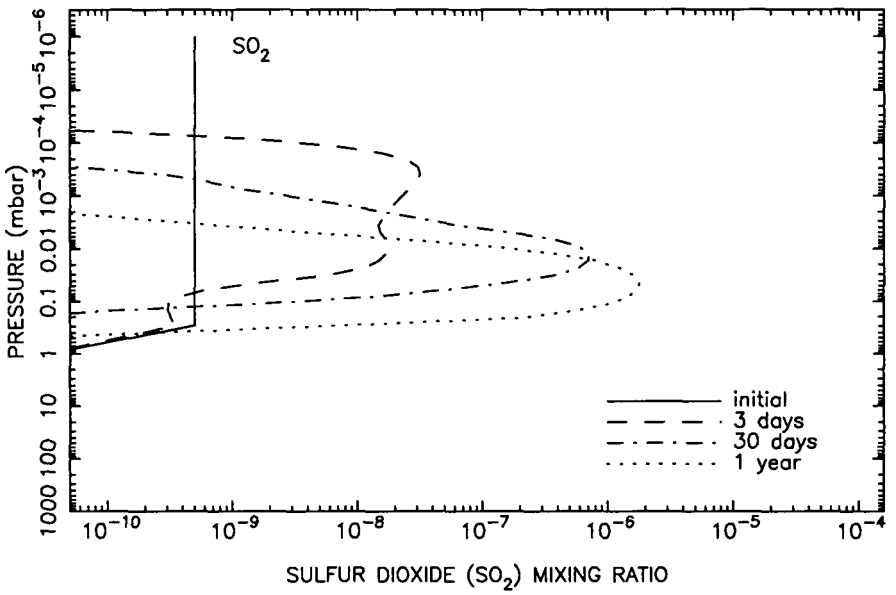

FIGURE 5. The photochemical evolution of SO_2 in Model C (from Moses *et al.* 1995c) in terms of the temporal variation of the SO_2 mixing ratio profile.

in the post-SL9 jovian stratosphere. Figures 6 & 7 illustrate the temporal variation of the partitioning of nitrogen among the different nitrogen compounds. Note that in both models, N_2 is the major reservoir for the nitrogen after several months.

The $(\tilde{A}\text{–}\tilde{X})$ band system of NH_3 lies in the 170–220 nm region. At these wavelengths, the primary photolysis pathway is $NH_2 + H$. The photolysis lifetime of NH_3 is ~ 5.7 days at 10^{-3} mbar—a time scale considerably longer than that for most of the active sulfur species. In the photochemical models, the NH_2 radicals formed by ammonia photolysis react with sulfur radicals such as S, SH, CS, and NS to either recycle the ammonia, to form N_2 and HCN, or to form nitrogen-sulfur species such as HNS, NS, and HNCS (see Section 4.1). In Model C, NS radicals are allowed to cluster together to form $(NS)_2$ and $(NS)_4$, which also become important reservoirs for the nitrogen and sulfur (see figure 7). The reactions of NH_2 with sulfur radicals cause the ammonia to be recycled less efficiently than otherwise might be the case and cause hydrazine (N_2H_4) formation to be suppressed.

As mentioned in the previous section, all these proposed sulfur-nitrogen reactions are hypothetical; none have been studied in the laboratory. Searches for potentially important species such as NS and HNCS at ultraviolet through microwave wavelengths (or even quoted upper limits) would greatly help in distinguishing between several possible pathways in the ammonia photochemistry. Note that these species take days or weeks to build up into potentially observable quantities. Failing such direct observational constraints, the observed lifetime of the NH_3 at the impact sites might help determine whether such proposed reactions are occurring.

One very noticeable difference between Models A & C is the apparent lifetime of NH_3 in the middle and lower stratosphere (cf. figures 6 & 7). The greater NH_3 lifetime in Model C has nothing to do with the increased abundance of oxygen compounds in that model; instead, the culprit is increased shielding by other molecules and, more importantly, by dust. Both CS_2 and H_2S absorb in the same wavelength region as NH_3. CS_2 is not abundant enough to markedly affect ammonia photolysis. If H_2S and NH_3 are

https://doi.org/10.1017/S0252921100115532 Published online by Cambridge University Press

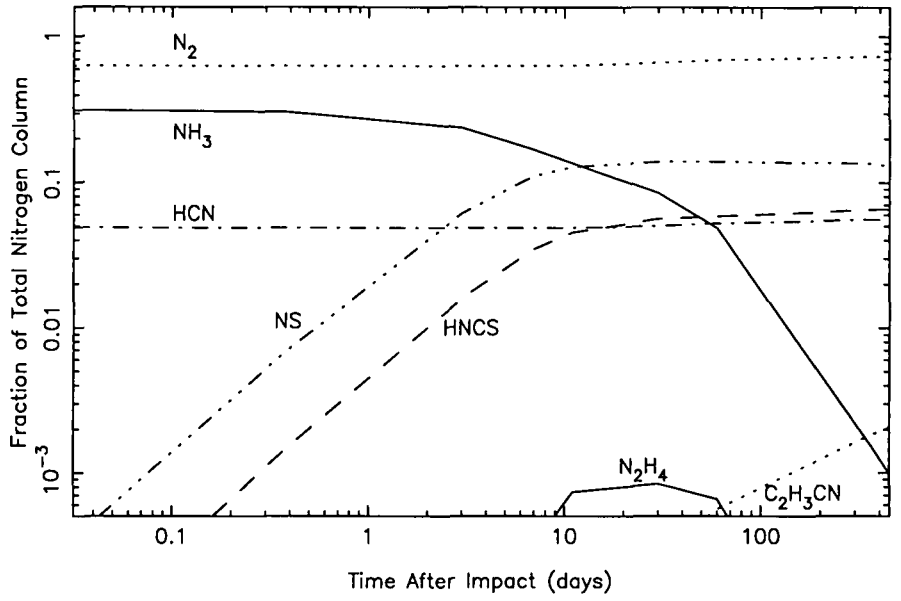

FIGURE 6. The time variation of the partitioning of nitrogen compounds in Model A (Moses *et al.* 1995b). The ordinate represents the fraction of the total nitrogen column (in terms of N atoms) that is contributed by the various molecules.

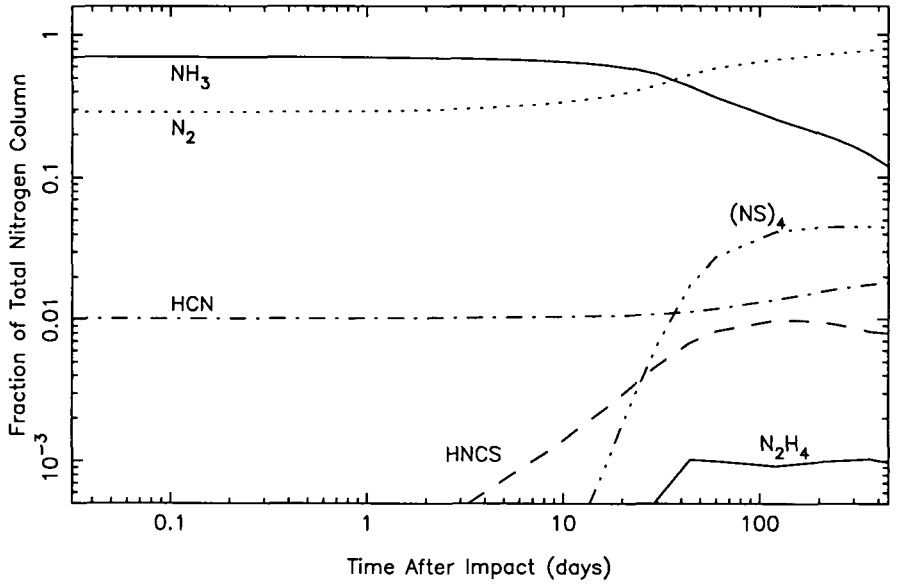

FIGURE 7. The time variation of the partitioning of nitrogen compounds in Model C (Moses *et al.* 1995c). The ordinate represents the fraction of the total nitrogen column (in terms of N atoms) that is contributed by the various molecules.

https://doi.org/10.1017/S0252921100115532 Published online by Cambridge University Press

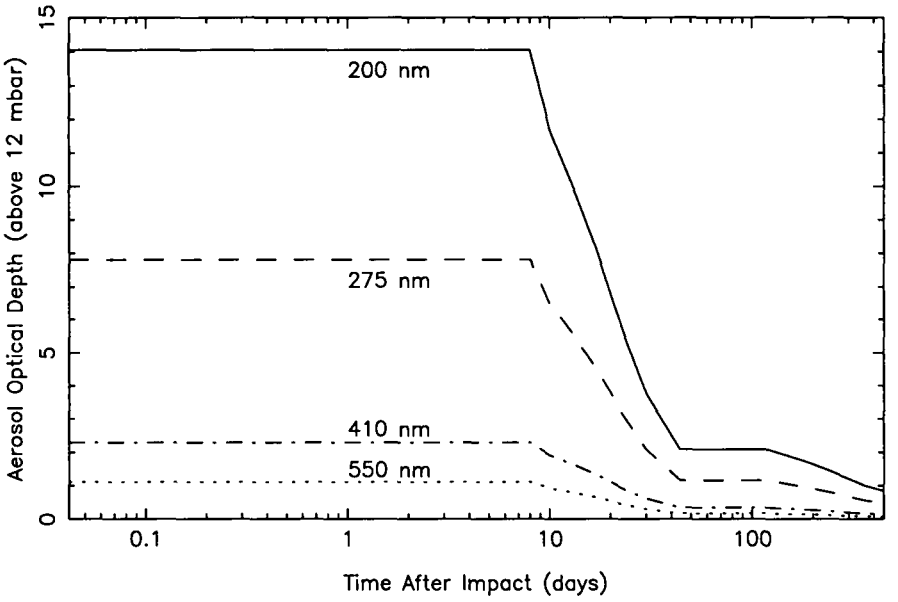

FIGURE 8. Time variation of aerosol opacity in Model C (Moses *et al.* 1995c)

co-located, as Yelle & McGrath (1996) suggest, then H_2S could be a potentially effective UV shield as long as the H_2S persists in the lower stratosphere. The dark widespread dust observed at the impact sites (*e.g.*, West *et al.* 1995) might also inhibit the penetration of ultraviolet radiation into the lower stratosphere. Several studies of the aerosol debris generated by the impacts suggest that the dust extends up to at least 0.3 mbar or perhaps even higher (*e.g.*, West *et al.* 1995, Mallama *et al.* 1995). If so, then this debris could affect ammonia photolysis.

To determine the effect of dust on the photochemistry, Moses *et al.* (1995c) add aerosol extinction to Model C and use a Mie scattering code to estimate dust opacities. The dust absorption cross sections are derived by assuming a log-normal distribution of spherical particles with a distribution width of 1.2 and a mean radius of 0.15 μm (the radius was chosen to be consistent with the dust analysis of F. Moreno *et al.* 1995 and Ortiz *et al.* 1995). The particle imaginary index of refraction was assumed to be typical of outer planetary hazes; *i.e.*, $k = \exp[-2.1 - 6.5 * \lambda(\mu\text{m})]$ and is consistent with the derived ultraviolet imaginary refractive indices of West *et al.* (1995). The dust number densities were chosen so that the haze opacity remains approximately consistent with the West *et al.* UV-visible optical depths. The initial dust profile adopted in Model C has a constant dust density of $\sim 8 \times 10^3$ particles cm^{-3} below 10 mbar, a dust number mixing ratio of 1.8×10^{-14} between 10–10^{-2} mbar and 10^{-25} above 10^{-2} mbar. Since West *et al.* (1995) demonstrate that the dust opacity decreases with time, Moses *et al.* (1995c) allow the dust number density to be reduced over time; however, the reduction in haze abundance was instituted somewhat arbitrarily. The resulting time variation in the haze opacity is shown in figure 8. Although not shown in the figure, the ratio of the dust opacities at 275 and 893 nm derived from this haze model is not quite consistent with the West *et al.* (1995) results. In addition, the haze model of F. Moreno *et al.* (1995) and Ortiz *et al.* (1995) would not be optically thick in the ultraviolet using the optical properties extrapolated from West *et al.* (1995). Both of these results suggest that the particles are indeed larger than 0.15 μm in radius, as indicated by West *et al.*

https://doi.org/10.1017/S0252921100115532 Published online by Cambridge University Press

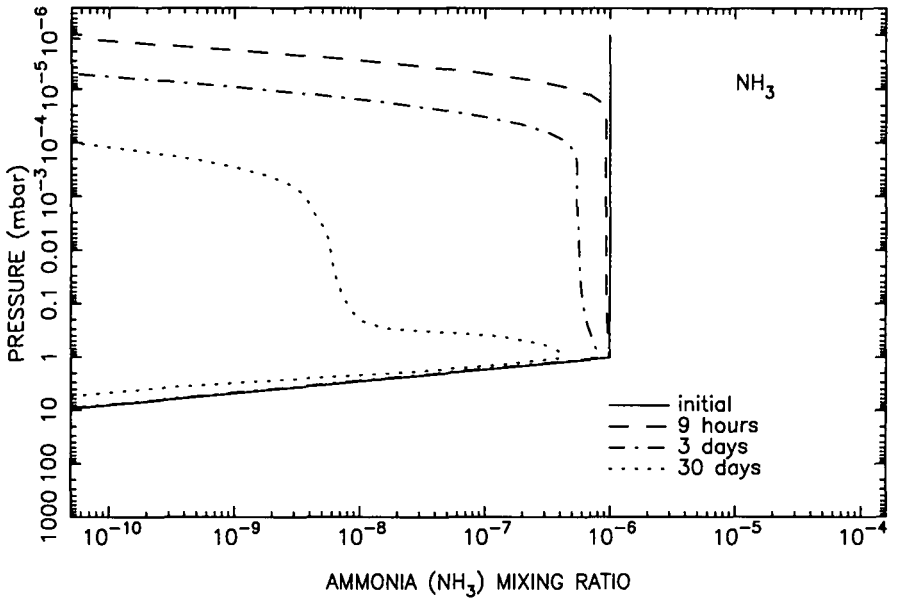

FIGURE 9. The photochemical evolution of NH_3 in Model A (from Moses *et al.* 1995a) in terms of the temporal variation of the NH_3 mixing ratio profile.

Figure 9 illustrates how the NH_3 profile varies with time in Model A. In the middle and upper stratosphere ($P < 10^{-2}$ mbar), the ammonia profile in Model C is virtually identical to that of Model A. However, absorption of solar radiation by dust keeps more NH_3 in the lower stratosphere in Model C. The haze optical depth in Model C is still ~ 1 at 1 mbar 10 days after the impacts and remains high for several weeks. Therefore, the dust provides an effective shield for the ammonia at low altitudes and prevents the NH_3 from being lost as rapidly as it normally would be. As will be discussed in Section 5, the fact that the NH_3 stays in the stratosphere in Model C much longer than is indicated by the observations suggests that the actual dust deposited by the impacts is not optically thick at millibar pressure levels in the near ultraviolet. Thus, the photochemical models can be used in conjunction with observations to place constraints on the stratospheric aerosol profile.

Hydrogen cyanide does not absorb near-ultraviolet radiation and only absorbs weakly below 190 nm. In addition, no chemical loss mechanisms are effective at removing HCN from Jupiter's stratosphere. Moses *et al.* (1995b) find that in Model A, the HCN formed during the plume splashdown is photochemically stable throughout the stratosphere, and they suggest that HCN might therefore be regarded as a good "thermometer" for the stratosphere—changes in the HCN observations might be due to temperature variations or horizontal spreading rather than to changes in total abundance. Moses *et al.* (1995c) derive a slightly different result for Model C. They see an increase in the HCN abundance over time due to the following series of reactions:

https://doi.org/10.1017/S0252921100115532 Published online by Cambridge University Press

$$
\begin{aligned}
NH_3 &\xrightarrow{h\nu} NH_2 + H \\
NH_2 + S &\longrightarrow HNS + H \\
HNS + H &\longrightarrow H_2 + NS \\
NS &\xrightarrow{h\nu} N + S \\
CH_3 + N &\longrightarrow H_2CN + H \\
H_2CN + H &\longrightarrow HCN + H_2 \\
\hline
\text{Net: } NH_3 + CH_3 &\longrightarrow HCN + 2H_2 + H
\end{aligned}
$$

Because NH_3 is initially so much more abundant than HCN in Model C, and because NS photolysis has been included, the increase in HCN abundance is more noticeable in Model C than in Model A.

Molecular nitrogen was probably an important reservoir for the nitrogen after the impact and the plume re-entry shocks (Zahnle 1996, Lyons & Kansal 1996). Its presence in the post-SL9 jovian stratosphere is inferred from the fact that the O/N ratio of the observed molecules at the impact sites is greater than that of typical comets, suggesting that N_2 might make up the "missing" nitrogen component (*e.g.*, Lellouch 1996). N_2 has no efficient photochemical loss mechanisms in the jovian stratosphere. The N_2 abundance increases with time in the photochemical models due to schemes such as the following:

$$
\begin{aligned}
2(NH_3 &\xrightarrow{h\nu} NH_2 + H) \\
NH_2 + S &\longrightarrow HNS + H \\
HNS &\xrightarrow{h\nu} H + NS \\
NH_2 + NS &\longrightarrow N_2 + H_2S \\
\hline
\text{Net: } 2NH_3 + S &\longrightarrow N_2 + H_2S + 4H
\end{aligned}
$$

Moderate amounts of hydrazine (N_2H_4) and nitriles such as acrylonitrile (C_2H_3CN) build up at various times in the photochemical models (see figures 6 & 7). However, it's not clear that these species can build up in observable quantities.

None of the nitrogen-bearing molecules in the photochemical models are predicted to contribute much mass to the stratospheric aerosol layer. Hydrazine may be abundant enough to condense after several months, and species with uncertain vapor pressures such as $(NS)_x$ clusters or rings may also condense in the stratosphere. If ammonia is as abundant initially in the deep stratosphere as is assumed in Model C, then NH_3 is close to its saturation vapor curve in the lower stratosphere, but there are indications that the initial NH_3 abundance in Model C may be an overestimate (see Section 5).

4.3. *Oxygen*

Interest in the chemistry of the Earth's stratosphere has motivated many laboratory studies of oxygen photochemistry, and most of the rate constants for the oxygen reactions in the Moses *et al.* models are well known. Initial conditions for the oxygen compounds at the impact sites are less certain; CO, H_2O, and OCS are the only oxygen-bearing molecules that have been identified. Figure 10 illustrates how these and other potentially important oxygen compounds vary with time. Note that CO and H_2O are much more photochemically stable than most of the sulfur-bearing molecules or ammonia. Since Model C is the only one that contains a non-trivial initial amount of water, it will be the focus of our discussion in this section.

Water photolysis drives the oxygen photochemistry. Photolysis of H_2O occurs at short wavelengths (*e.g.*, $\lambda < 190$ nm); thus, H_2O is relatively stable in Jupiter's stratosphere. Its photolysis lifetime is almost 3 months at 10^{-3} mbar in Model C. In addition, H_2O is recycled to a large degree once it is photolyzed. The OH reacts with H_2 to reform water. However, some of the OH radicals react with S to form SO or react with SO to form

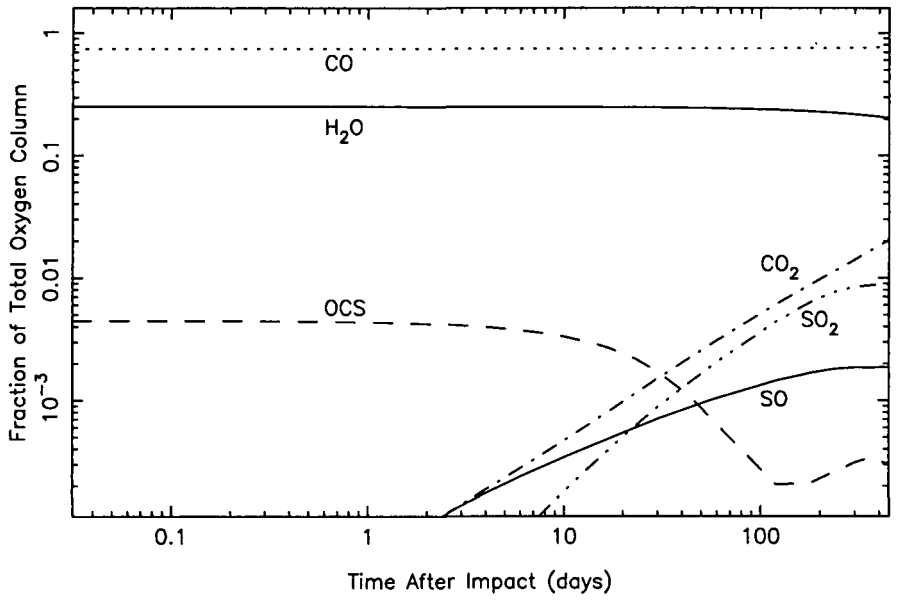

FIGURE 10. The time variation of the partitioning of oxygen compounds in Model C (Moses *et al.* 1995c). The ordinate represents the fraction of the total oxygen column (in terms of O atoms) that is contributed by the various molecules.

SO_2 so that the abundances of sulfur monoxide and sulfur dioxide increase with time. Another interesting loss process is OH + CO $\longrightarrow$ CO_2 + H. This reaction is slow and barely makes a dent in the CO abundance after 1 year; however, the reaction does cause the carbon dioxide (CO_2) abundance to increase noticeably with time (see figure 10).

Theoretical models predict that large quantities of CO will form during both the initial impact explosion and the plume splashdown for virtually all possible composition, temperature, and pressure conditions assumed for the shocks (Zahnle 1996, Lyons & Kansal 1996). Carbon monoxide is photochemically stable, and Moses *et al.* (1995a,b,c) suggest that CO might be a good tracer for temperature changes or atmospheric dynamics after the impacts. In the photochemical models, CO is the ultimate repository for most of the oxygen compounds. For instance, CO is produced directly by OCS and CO_2 photolysis, and indirectly by H_2O, SO, and SO_2 photolysis. Schemes such as the following are effective at converting H_2O to CO:

$$\begin{aligned}
H_2O &\xrightarrow{h\nu} OH + H \\
OH + S &\longrightarrow SO + H \\
SO &\xrightarrow{h\nu} S + O \\
O + CH_3 &\longrightarrow H_2CO + H \\
H_2CO + H &\longrightarrow HCO + H_2 \\
HCO + H &\longrightarrow CO + H_2 \\
\hline
\text{Net: } H_2O + CH_3 &\longrightarrow CO + 2H_2 + H
\end{aligned}$$

Note that formaldehyde (H_2CO) is an intermediary in the above reaction. Moderate amounts (*e.g.*, 10^{13}–10^{15} molecules cm^{-2}) of H_2CO, methanol (CH_3OH), and nitric oxide (NO) form in the photochemical model after a week or so. Other important oxygen-bearing molecules include OCS, SO, SO_2, and $(SO)_2$. A discussion of the photochemistry of these molecules is included in Section 4.1.

https://doi.org/10.1017/S0252921100115532 Published online by Cambridge University Press

None of the oxygen compounds are expected to be abundant enough to condense in the lower stratosphere. It is interesting to note, however, that the initial H_2O abundance selected for Model C puts H_2O very close to its saturation point in the lower stratosphere. No other oxygen compounds in the model are even close to saturation within a period of 15 months after the impacts.

5. Model-data comparisons

To determine if the chemical state of the atmosphere has responded as expected to the impacts, we compare the photochemical model predictions with observational data. The record of the time variation of the different observed molecules is particularly useful in determining physical and chemical conditions at the impact sites and in helping to constrain some of the uncertain initial conditions and chemical reaction schemes. Information about the temporal variation of at least 7 of the observed molecules (*e.g.*, S_2, CS_2, CS, OCS, NH_3, HCN, CO, and perhaps H_2S) has been presented in the literature. We will discuss each of these molecules and evaluate whether the photochemical models are consistent with the observations. Remember that the photochemical models are one-dimensional; because horizontal spreading is ignored, the models should always overpredict column abundances at later times.

As discussed by Noll *et al.* (1995), S_2 absorption lines were seen in the HST FOS spectra of the G impact site on July 18, 1994 ($\sim$ 3.5 hours after the G impact) and on July 21, 1994 ($\sim$ 3 days after the G impact, but only 45 minutes after the nearby S impact). The viewing geometry of the observations was not the same in the two cases, and the S_2 signature in the July 21 spectra may be due to S_2 at the G impact site, or it may be due to S_2 at the smaller, but more recent, S impact site. No S_2 absorption lines were observed on August 9, 1994 (22 days later) or at any time after July 21, 1994 (Noll *et al.* 1995, McGrath *et al.* 1995).

In the Moses *et al.* (1995a) photochemical model (Model A), the S_2 abundance drops by a factor of $\sim$ 20 in the first month after the impacts; however, most of that reduction occurs in the first day. (Note that the S_8 shown in figures 1 & 2 is directly derived from S_2). Between 3 days and 30 days, the S_2 column decreases by only a factor of $\sim$ 2. If the July 21 signature is due to the presence of S_2 at the fresh S site rather than at the 3-day-old G site, then Model A may be consistent with observations. On the other hand, if the July 21 signature is due to S_2 at the G impact site, then Model A probably overpredicts the rate of loss of S_2 at the impact sites.

A straightforward decrease in the assumed initial S_2 abundance at all altitudes in the photochemical model allows the S_2 to remain in the stratosphere for a longer period of time. However, in that situation, the S_2 probably persists too long to account for observations. For instance, in Model C, the S_2 column drops by only a factor of $\sim$3 in the first 23 days. Although no upper limits are given in Noll *et al.* (1995) or McGrath *et al.* (1995) for the August 9, 1994 data, the observations probably indicate a more dramatic decrease in the S_2 abundance than is seen in Model C.

A cautionary note needs to be inserted here with regard to the photochemical modeling of S_2. The S_2 may initially be confined to higher altitudes than is assumed in the photochemical models (see Yelle & McGrath 1995), and the photochemistry of S_2 is not well understood. More importantly, the photochemical models are diurnally averaged. S_2 and the other sulfur radicals have short photochemical lifetimes, and diurnally averaged models may not truly represent the situation at the impact sites. Further comparisons between S_2 observations and models should be delayed until more appropriate photochemical models are developed.

CS_2 is always seen in ultraviolet spectra of the impact sites, even 9 months after the impacts (McGrath *et al.* 1995). This result is consistent with both of the photochemical models of Moses *et al.* who find that reactions between sulfur and hydrocarbon radicals produce CS_2 in the mid-to-lower stratosphere several months after the impacts. Both Model A and C predict that CS_2 will be readily photolyzed and lost from the upper atmosphere; however, a slower rate of decline in the total CS_2 column is predicted in Model C relative to Model A. Model A exhibits a total drop in the CS_2 column of a factor of 40 in the first 30 days while Model C predicts that the CS_2 column would have decreased by a factor of 2.5 between the July 18 and the August 9 observations and by just a factor of $\sim$ 3 between July 18 and August 23, 1994. The actual observations seem consistent with the Model C results but inconsistent with the Model A results. Yelle & McGrath (1996) derive a decrease in the CS_2 column of a factor of 2–3 between July 18 and August 9, and another factor of $\sim$2 between August 9 and August 23. The persistence of CS_2 in the observations suggests that some shielding is going on (*e.g.*, from dust or from NH_3) as in Model C or that CS_2 is more efficiently recycled or produced than is evident in Model A.

One interesting prediction from Model C is that the CS_2 will end up being co-located with the stratospheric NH_3 weeks or months after the impacts. Yelle & McGrath (1996) suggest that the bulk of the CS_2 is originally located at higher altitudes than the ammonia. However, Moses *et al.* find that CS_2 disappears from the upper stratosphere over time but persists in a similar altitude region as the NH_3. It will be interesting to see whether an analysis of the FOS spectra taken in August, 1994 will support this prediction.

CS has been monitored on a regular basis at millimeter and submillimeter wavelengths from the IRAM and JCMT telescopes (Lellouch *et al.* 1995, R. Moreno *et al.* 1995, Matthews *et al.* 1995). Six to twelve months after the impacts, the CS column abundance appears to be $\sim$ 10 times less than in July 1994 (Moreno *et al.* 1995, Matthews *et al.* 1995, Lellouch 1996). If we follow the arguments of Lellouch (1996) and assume that the spots have spread by a factor of $\sim$ 80 in area in this time, then the data imply that the total CS mass may have increased by a factor of $\sim$ 8 during the 6–12 month period following the impacts.

Both Models A and C exhibit a steady increase in the CS column abundance in the weeks and months following the impacts. In Model A, a factor of 20 increase in the CS column is predicted between 1 week and 1 year after the impacts. In Model C, a factor of 80 increase is predicted between 1 week and 1 year. Both models grossly overestimate the increase of the CS column with time. Because the CS in the photochemical models is derived from S_2 photochemistry, the inconsistencies between models and data suggest that the models overestimate the initial S_2/CS ratio. In fact, Moses *et al.* (1995a,b,c) do not begin with much CS at all (see Table 1), mainly because some of the original thermochemical models (*e.g.*, Zahnle *et al.* 1995) did not favor CS production and because the initial large S_2 abundance in Model A allowed a substantial build-up in the CS abundance after a day or so (*i.e.*, large initial amounts of CS were not required to explain the observations). If $S_2/CS \lesssim 1$ initially, then the photochemical models would not show such a dramatic increase in the CS abundance with time unless some other sulfur compound is present in much larger quantities than CS.

OCS was detected at mm wavelengths at the IRAM telescope on July 22, 1994 (Lellouch *et al.* 1995). The detection was not confirmed at the same telescope 1 month later (Lellouch 1996). Photochemical models predict that OCS is lost at a steady rate in the jovian stratosphere due to photolysis at near-ultraviolet wavelengths (with a photolysis lifetime of 24 days). Dust helps shield the OCS from photolysis in the Model C; even

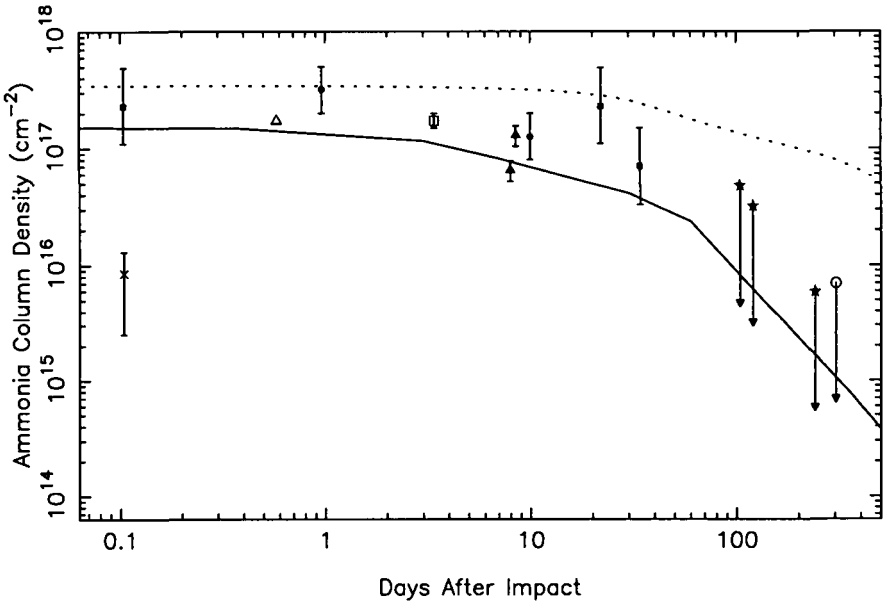

FIGURE 11. The time variation of NH_3 (after Fast *et al.* 1995). The solid line represents the photochemical model results of Model A, and the dotted line the results of Model C. Observations are indicated by individual points and associated error bars. The cross is from Atreya *et al.* (1995), the solid squares from Yelle & McGrath (1996) (where the range is calculated assuming the NH_3 is confined between 5 mbar and either 12 or 40 mbar), the open triangle from Conrath *et al.* (1995, personal communication to T. Kostiuk), the solid circles from Griffith *et al.* (1995a), the open square from Betz *et al.* (1995), the solid triangles from Kostiuk *et al.* (1995), the solid stars (upper limits) from Fast *et al.* (1995), and the open circle (upper limit) from Bézard *et al.* (1995). Note: Most of the observations are quoted for columns above 40–150 mbar; the Atreya *et al.* values are for the column above 0.3–10 mbar. Note also that observations made in the first few weeks were often centered at different impact sites.

so, the model predicts a factor of ~ 2.6 decrease in the OCS column after 30 days. This decrease may be consistent with the observations (Lellouch 1996).

Although the H_2S detection is controversial, Yelle & McGrath (1996) suggest that H_2S is present in the HST FOS spectra 3.5 hours after the impact, but not 22 days later. This suggestion is consistent with photochemical models.

The time variation of ammonia has been monitored extensively at infrared and ultraviolet wavelengths. Figure 11 shows how the photochemical model results compare with observations. Observations taken many months after the impacts show no evidence for NH_3 in the middle and upper stratosphere (Fast *et al.* 1995, Bézard *et al.* 1995). However, NH_3 is visible in ultraviolet spectra taken 9 months after the impacts (McGrath *et al.* 1995), suggesting that NH_3 may still be enhanced in the lower stratosphere and/or upper troposphere relative to pre-impact values. This latter conclusion will not be confirmed until the data are fully analyzed. As discussed in Section 4.2, the observed time variation of NH_3 appears more consistent with Model A than Model C, suggesting that too much dust shielding has been included in the latter model. If we take the models at face value, the model-data comparisons tell us that the dust cannot be optically thick above a few mbar a week or so after the impacts. However, keep in mind that horizontal spreading has not been included in the photochemical models. It is not clear how fast the material at a few mbar to a few 10's of mbar (where most of the NH_3 is located

according to the infrared observations) is spreading. If there is a factor of $\sim$ 80 areal spreading 6–12 months after the impacts compared with the spot size during the week of the impacts, then Model C may easily be consistent with observations.

HCN, like CS, has been monitored at millimeter and submillimeter wavelengths on a regular basis (Marten *et al.* 1995, Matthews *et al.* 1995). The HCN column abundance has appeared to drop by a factor of $\sim$ 10 in the 6–12 months following the impacts (Matthews *et al.* 1995, R. Moreno *et al.* 1995). If horizontal spreading is assumed to have caused the areal extent of the impact sites to increase by a factor of $\sim$ 80, then the mm and sub-mm observations indicate that the HCN abundance (*e.g.*, total mass) may have increased by as much as a factor of $\sim$ 8 over time. IRTF/IRSHELL 10-μm observations also indicate that HCN persists in the jovian stratosphere and that the total HCN mass may have increased in the 10 months following the impacts (Griffith *et al.* 1995b).

These results are consistent with the suggestion of Moses *et al.* that HCN is produced from NH_3 photolysis. The relative increase in the total HCN column depends on the initial NH_3/HCN ratio. To produce HCN, the photochemical models require a source of atomic nitrogen. In the Moses *et al.* models, N is supplied by speculative reactions involving ammonia photolysis products and sulfur, and have NS as an intermediate. Positive or negative searches for NS and other nitrogen-sulfur molecules in observational data would help constrain possible chemical pathways for the production of HCN.

The molecule with the most surprising observed temporal variation as compared with photochemical models is CO. Millimeter and submillimeter observations in the year following the impacts indicate that the impact sites have a CO column abundance that is $\sim$ 160 times less than in July, 1994 (R. Moreno *et al.* 1995, Matthews *et al.* 1995, Lellouch 1996). When spreading is taken into account, the implied reduction in total abundance (mass) is a factor of $\sim$ 2. Photochemical models do not reproduce a loss of this magnitude loss over the course of a year. In fact, Model C predicts that the CO abundance will increase with time due to H_2O photolysis products reacting with hydrocarbons to form CO. Lellouch (1996) discusses this problem in detail.

How could CO decrease with time while HCN and CS do not? One possible way to reconcile the problem is to assume that the bulk of the CO is located at a different altitude than that of the CS and HCN. In that case, the temperature variation and rate of horizontal spreading may be different. For instance, HCN and CS are favored by moderately shocked conditions in a "dry" plume; *i.e.*, one that has C/O $>$ 1 (Zahnle 1996, Lyons & Kansal 1996). If the oxygen is derived from the comet rather than from the jovian atmosphere, then much of the CO may have come from a different region of the plume/fireball (*i.e.*, one with C/O $<$ 1) and hence may have been deposited in a different altitude region during the plume splashback. Zahnle (1996) suggests that the cometary material may have been shocked to very high temperatures, and thus represents the material that has been flung the farthest and deposited the highest in the atmosphere. In addition, the molecules may be filling different areal fractions of the observed impact "scars." One can then imagine scenarios in which the CO spreads and dilutes more rapidly than the CS or HCN. One problem with such scenarios is that the altitudes derived from the millimeter observations (R. Moreno *et al.* 1995) are similar for the CO, CS, and HCN, and we know that HCN has spread over a large area (Griffith *et al.* 1995b).

Alternatively, some loss mechanism for the CO that has not been included in the Moses *et al.* photochemical models may be present in the jovian atmosphere. If the reduction in the CO abundance is due to photochemical processes, then observations should show a corresponding increase in some other oxygen compound such as CO_2, SO_2, or NO (unless

the CO is converted to something that will condense in the stratosphere). No increase in any other oxygen compounds have been found, but it is not clear that anyone has been looking. Recently ($\sim$ 15 months after the impacts), IRAM observations taken under good seeing conditions showed no evidence for SO_2 in the jovian stratosphere (E. Lellouch and R. Moreno, personal communication).

6. Conclusions

The collision of comet Shoemaker-Levy 9 with Jupiter resulted in profound changes to the jovian atmosphere. To fully understand the chemical changes that occurred after the impacts, photochemical models of the post-SL9 jovian stratosphere have been developed (Moses *et al.* 1995a,b,c). These models are used to trace chemical changes over time and to connect observations taken days or weeks after the impacts with chemical abundances at the time of the plume splashdown.

The theoretical models indicate that the photochemistry at the impact sites is rapid and complex. The sulfur species introduced by the impacts evolve very quickly. Condensed S_8 is the main reservoir for the sulfur over time, and the aerosols should become progressively coated with sulfur compounds (*e.g.*, S_8, H_2S_x, N–S and C–S polymers). One important prediction, that the CS abundance persists with time, seems to be supported by mm and sub-mm observations (R. Moreno *et al.* 1995, Matthews *et al.* 1995); however, the dramatic increase of the modeled CS abundance with time is not mirrored in the observations, indicating that the initial S_2/CS ratio at the impact sites was probably $\lesssim 1$. The observed abundances of CS_2, OCS, and perhaps H_2S all seem to decrease roughly as expected. Two predictions remain to be investigated: (1) unusual nitrogen-sulfur species such as NS and HNCS are predicted to become important reservoirs for both the sulfur and the nitrogen at the impact sites, and (2) SO_2 will become an important reservoir for the sulfur if H_2O was an important initial constituent at the impact sites. Positive or negative searches for these molecules in data taken months after the impacts will help distinguish between several possible chemical schemes that may have occurred at the impact sites and will help constrain the initial water abundance.

Nitrogen compounds tend to be more stable at the impact sites than sulfur compounds. NH_3 photolysis, which operates on a week time scale, drives the nitrogen photochemistry. N_2 is predicted to be the main nitrogen reservoir over time. In the photochemical models, the HCN abundance increases slightly with time due to reactions catalyzed by sulfur radicals; the HCN observations appear to be consistent with this prediction (Matthews *et al.* 1995, R. Moreno *et al.* 1995, Griffith *et al.* 1995b). The observed rate of decrease of NH_3 may indicate that the dust introduced by the impacts was not optically thick at a few mbar at near-ultraviolet wavelengths after the first week of the impacts. This conclusion will not be firm until we have a better handle on the amount of horizontal spreading at the impact sites.

H_2O and CO are predicted to be very stable in the jovian stratosphere. Water, which has a photolysis lifetime of months, will drive the oxygen photochemistry. If large quantities of H_2O were present throughout the impact sites, then CO_2, SO_2, SO, and NO will become important oxygen reservoirs over time. The observed decrease in the CO abundance with time (R. Moreno *et al.* 1995, Matthews *et al.* 1995, Lellouch 1996) is not consistent with photochemical models. The models may be neglecting some scheme that converts the CO to other as-yet-unobserved oxygen compounds, or the CO may have been deposited at a different location than the HCN and CS and so may have experienced a different rate of horizontal spreading.

Improved photochemical models should help resolve some of the problems with the current model-data comparisons. More realistic initial vertical profiles for the different observed species can be developed now that more sophisticated observational analyses are being published. Future photochemical models should also include parameterizations to take horizontal spreading into account and should allow for diurnal variations. More extensive thermochemical modeling should also help constrain the initial conditions required for accurate photochemical modeling. The Shoemaker-Levy 9 impacts have provided us with a unique opportunity to observe some unusual atmospheric photochemistry in action; photochemical models can be valuable tools in interpreting the chemical evolution at the impact sites.

We thank R. Yelle, K. Zahnle, E. Lellouch, and M. Allen for thorough reviews of the manuscript and many useful discussions.

REFERENCES

ATREYA, S. K., EDGINGTON, S. G., TRAFTON, L. M., CALDWELL, J. J., NOLL, K. S., & WEAVER, H. A. 1995 Abundances of ammonia and carbon disulfide in the Jovian stratosphere following the impact of comet Shoemaker-Levy 9. *Geophys. Res. Lett.* **22**, 1625–1628.

BETZ, A. L., BOREIKO, R. T., BESTER, M., DANCHI, W. C., & HALE D. D. 1995 Stratospheric ammonia in Jupiter after the impact of comet SL-9. *Bull. Amer. Astron. Soc.* **26**, 1590–1591.

BÉZARD, B., GRIFFITH, C., GREATHOUSE, T., KELLY, D., LACY, J., & ORTON, G. 1995 Jupiter ten months after the collision of comet SL9: Stratospheric temperatures and ammonia distribution. *Bull. Amer. Astron. Soc.* **27**, 1126.

BJORAKER, G. L., HERTER, T., GULL, G., STOLOVY, S. & PIRGER, B. 1995 Detection of water in the "splash" of fragments G and K of comet Shoemaker-Levy 9. In *Abstracts for IAU Colloquium 156: The Collision of Comet P/Shoemaker-Levy 9 and Jupiter*, p. 8.

BORUNOV, S., DROSSART, P., ENCRENAZ, TH., & DOROFEEVA, V. 1995 Thermochemistry in the fireball of SL9 impacts. *Bull. Amer. Astron. Soc.* **27**, 1120.

BROOKE, T. Y., ORTON, G. S., CRISP, D., FRIEDSON, A. J. & BJORAKER, G. 1995 Near-infrared spectroscopy of the Shoemaker-Levy 9 impact sites with UKIRT: CO emission from the L site. In *Abstracts for IAU Colloquium 156: The Collision of Comet P/Shoemaker-Levy 9 and Jupiter*, p. 12.

CALDWELL, J., MARTYN, M., DELRIZZO, D., ATREYA, S., EDGINGTON, S., BARNET, C., NOLL, K., WEAVER, H., TRAFTON, L., & YOST, S. 1995 Upper limits on SiO, H_2S, C_2H_2 and H_2O on Jupiter from SL9. *Bull. Amer. Astron. Soc.* **27**, 1118–1119.

CARLSON, R. W., WEISSMAN, P. R., HUI, J., SEGURA, M., SMYTHE, W. D., BAINES, K. H., JOHNSON, T. V., DROSSART, P., ENCRENAZ, T., LEADER, F. & MEHLMAN, R. 1995 Galileo infrared observations of the Shoemaker-Levy 9 G and R fireballs and splash. In *Abstracts for IAU Colloquium 156: The Collision of Comet P/Shoemaker-Levy 9 and Jupiter*, p. 15.

CONRATH, B. J., GIERASCH, P. J., HAYWARD, T., MCGHEE, C. NICHOLSON, P. D. & VAN CLEVE, J. 1995 Palomar mid-infrared spectroscopic observations of comet Shoemaker-Levy 9 impact sites. In *Abstracts for IAU Colloquium 156: The Collision of Comet P/Shoemaker-Levy 9 and Jupiter*, p. 24.

COSMOVICI, C. B., MONTEBUGNOLI, S., POGREBENKO, S. & COLOM, P. 1995 Water MASER detection at 22 GHz after the SL-9/Jupiter collision. *Bull. Amer. Astron. Soc.* **27**, 1133.

FAST, K. E., LIVENGOOD, T. A., KOSTIUK, T., BUHL, D., ESPENAK, F., BJORAKER, G. L., ROMANI, P. N., JENNINGS, D. E., SADA, P., ZIPOY, D., GOLDSTEIN, J. J., & HEWEGAMA, T. 1995 NH_3 in Jupiter's stratosphere within the year following the SL9 impacts. *Bull. Amer. Astron. Soc.* **27**, 1126–1127.

GLADSTONE, G. R., ALLEN, M., & YUNG, Y. L. 1996 Hydrocarbon photochemistry in the upper atmosphere of Jupiter. *Icarus* **119**, 1–52.

GRIFFITH, C. A., BÉZARD, B., KELLY, D., LACY, J., GREATHOUSE, T., & ORTON, G. 1995a Mid-IR spectroscopy and NH_3 and HCN images of K impact site. In *Abstracts for IAU Colloquium 156: The Collision of Comet P/Shoemaker-Levy 9 and Jupiter*, p. 42.

GRIFFITH, C. A., BÉZARD, B., GREATHOUSE, T., KELLY, D., LACY, J., & ORTON, G. 1995b Jupiter ten months after the collision of comet SL9: Spectral maps of HCN and NH_3. *Bull. Amer. Astron. Soc.* **27**, 1126.

HEAL, H. G. 1972 The sulfur nitrides. *Adv. Inorg. Chem. Radiochem.* **15**, 375–412.

KIM, S. J., RUIZ, M., RIEKE, G. H., & RIEKE, M. J. 1995 Thermal history of the R impact flare of comet Shoemaker-Levy 9. *Bull. Amer. Astron. Soc.* **27**, 1120.

KNACKE, R. F., FAJARDO-ACOSTA, S. B., GEBALLE, T. R., & NOLL, K. S. 1995 Infrared spectroscopy of the R-impact of comet Shoemaker-Levy 9. *Bull. Amer. Astron. Soc.* **27**, 1114.

KOSTIUK, T., BUHL, D., ESPENAK, F., ROMANI, P., BJORAKER, G., FAST, K., LIVENGOOD, T., & ZIPOY, D. 1996 Stratospheric ammonia on Jupiter after the SL9 collision. *Icarus*, submitted.

LELLOUCH, E. 1996 Chemistry induced by the impacts: Observations. *This volume.*

LELLOUCH, E., PAUBERT, G., MORENO, R., FESTOU, M. C., BÉZARD, B., BOCKELÉE-MORVAN, D., COLOM, P., CROVISIER, J., ENCRENAZ, T., GAUTIER, D., MARTEN, A., DESPOIS, D., STROBEL, D. F., & SIEVERS, A. 1995 Chemical and thermal response of Jupiter's atmosphere following the impact of comet Shoemaker-Levy 9. *Nature* **373**, 592–595.

LYONS, J. R., & KANSAL, A. 1996 A chemical kinetics model for analysis of the comet Shoemaker-Levy 9 impacts with Jupiter. *Icarus*, submitted.

MAILLARD, J.-P., DROSSART, P., BÉZARD, B., DE BERGH, C., LELLOUCH, E., MARTEN, A., CALDWELL, J., HILICO, J.-C., & ATREYA, S. K. 1995 Methane and carbon monoxide infrared emissions observed at the Canada-France-Hawaii Telescope during the collision of comet SL-9 with Jupiter. *Geophys. Res. Lett.* **22**, 1573–1576.

MALLAMA, A., NELSON, P., & PARK, J. 1995 Detection of very high altitude fallout from the comet Shoemaker-Levy 9 explosions in Jupiter's atmosphere. *Geophys. Res. Lett.* **100**, 16,879–16,884.

MALLARD, W. G., WESTLEY, F., HERRON, J. T., HAMPSON, R. F., & FRIZZELL, D. H. 1994 NIST Chemical Kinetics Database—Version 6.0. *NIST Standard Reference Data*, Gaithersburg, MD.

MARTEN, A., GAUTIER, D., GRIFFIN, M. J., MATTHEWS, H. E., NAYLOR, D. A., DAVIS, G. R., OWEN, T., ORTON, G., BOCKELÉE-MORVAN, D., COLOM, P., CROVISIER, J., LELLOUCH, E., DE PATER, I., ATREYA, S., STROBEL, D., HAN, B., & SANDERS, D. B. 1995 The collision of comet Shoemaker-Levy 9 with Jupiter: Detection and evolution of HCN in the stratosphere of the planet. *Geophys. Res. Lett.* **22**, 1589–1592.

MATTHEWS, H. E., MARTEN, A., GRIFFIN, M. J., OWEN, T., & GAUTIER, D. 1995 JCMT observations of long-lived molecules on Jupiter in the aftermath of the comet Shoemaker-Levy 9 collision. *Bull. Amer. Astron. Soc.* **27**, 1121.

MCGRATH, M. A., YELLE, R. V., NOLL, K. S., WEAVER, H. A., & SMITH, T. E. 1995 Hubble Space Telescope spectroscopic observations of the Jovian atmosphere following the SL9 impacts. *Bull. Amer. Astron. Soc.* **27**, 1118.

MEADOWS, V. S., & CRISP, D. 1995 Near-infrared imaging spectroscopy of the impacts of SL9 fragments C, D, G, K, N, R, V, and W with Jupiter. *Bull. Amer. Astron. Soc.* **27**, 1127.

MOLTZEN, E. K., KLABUNDE, K. J., & SENNING, A. 1988 Carbon monosulfide: A review. *Chem. Rev.* **88**, 391–406.

MORENO, F., MUÑOZ, O., MOLINA, A., LÓPEZ-MORENO, J. J., ORTIZ, J. L., RODRÍGUEZ, J., LÓPEZ-JIMÉNEZ, A., GIRELA, F., LARSON, S. M., & CAMPINS, H. 1995 Physical properties of the aerosol debris generated by the impact of fragment H of comet P/Shoemaker-Levy 9 on Jupiter. *Geophys. Res. Lett.* **22**, 1609–1612.

MORENO, R., MARTEN, A., LELLOUCH, E., PAUBERT, G., & WILD, W. 1995 Long-term evolution of CO and CS in the Jupiter stratosphere after the comet Shoemaker-Levy 9 collision: Millimeter observations with the IRAM–30m telescope. *Bull. Amer. Astron. Soc.* **27**, 1129.

MOSES, J. I., ALLEN, M., & GLADSTONE, G. R. 1995a Post-SL9 sulfur photochemistry on Jupiter. *Geophys. Res. Lett.* **22**, 1597–1600.

MOSES, J. I., ALLEN, M., & GLADSTONE, G. R. 1995b Nitrogen and oxygen photochemistry following SL9. *Geophys. Res. Lett.* **22**, 1601–1604.

MOSES, J. I., ALLEN, M., FEGLEY, B., JR., & GLADSTONE, G. R. 1995c Photochemical evolution of the post-SL9 Jovian stratosphere. *Bull. Amer. Astron. Soc.* **27**, 1119.

NICHOLAS, J. E., AMODIO, C. A., & BAKER, M. J. 1979 Kinetics and mechanism of the decomposition of H_2S, CH_3SH and $(CH_3)_2S$ in a radio-frequency pulse discharge. *J. Chem. Soc. Faraday Trans. 1* **75**, 1868–1875.

NOLL, K. S., MCGRATH, M. A., TRAFTON, L. M., ATREYA, S. K., CALDWELL, J. J., WEAVER, H. A., YELLE, R. V., BARNET, C., & EDGINGTON, S. 1995 HST spectroscopic observations of Jupiter after the collision of Comet Shoemaker-Levy 9. *Science* **267**, 1307–1313.

ORTIZ, J. L., MUÑOZ, O., MORENO, F., MOLINA, A., HERBST, T. M., BIRKLE, K., BÖHNHARDT, & HAMILTON, D. P. 1995 Models of the SL-9 collision-generated hazes. *Geophys. Res. Lett.* **22**, 1605–1608.

ORTON, G. & 57 CO-AUTHORS. 1995 Collision of comet Shoemaker-Levy 9 with Jupiter observed by the NASA Infrared Telescope facility. *Science* **267**, 1277–1282.

SPRAGUE, A. L., BJORAKER, G. L., HUNTEN, D. M., WITTEBORN, F. C., KOZLOWSKI, R. W. H. & WOODEN, D. H. 1995. Water brought into Jupiter's atmosphere by fragments R and W of comet SL-9 *Icarus*, in press.

TURNER, B. E. 1989. Recent progress in astrochemistry. *Space Sci. Rev.* **51**, 235–337.

WEST, R. A., KARKOSCHKA, E., FRIEDSON, A. J., SEYMOUR, M., BAINES, K. H. & HAMMEL, H. B. 1995 Impact debris particles in Jupiter's stratosphere. *Science* **267**, 1296–1301.

YANG, S. C., FREEDMAN, A., KAWASAKI, M., & BERSOHN, R. 1980 Energy distribution of the fragments produced by photodissociation of CS_2 at 193 nm. *J. Chem. Phys.* **72**, 4058–4062.

YELLE, R. V., & MCGRATH, M. A. 1995 Results from HST spectroscopy of the SL9 impact sites. *Bull. Amer. Astron. Soc.* **27**, 1118.

YELLE, R. V., & MCGRATH, M. A. 1996 Ultraviolet spectroscopy of the SL9 impact sites. I. The 175–230 nm region. *Icarus* **119**, 90–111.

ZAHNLE, K. 1995 Dynamics and chemistry of SL9 plumes. *This volume.*

ZAHNLE, K., MAC LOW, M.-M., LODDERS, K., & FEGLEY, B., JR. 1995 Sulfur chemistry in the wake of comet Shoemaker-Levy 9. *Geophys. Res. Lett.* **22**, 1593–1596.